

## TRANSIENT PHENOMENA AND THEIR CONSIDERATION IN LOAD-FOLLOWING CONTROL OF NUCLEAR POWER PLANTS

by

**Pal SZENTANNAI<sup>a,b\*</sup>, Tibor SZUCS<sup>a</sup>,  
Balint PUDLEINER<sup>a,b</sup>, and Tamas FEKETE<sup>a</sup>**

<sup>a</sup> Centre for Energy Research, Budapest, Hungary

<sup>b</sup> Department of Energy Engineering, Faculty of Mechanical Engineering,  
Budapest University of Technology and Economics, Budapest, Hungary

Original scientific paper

<https://doi.org/10.2298/TSCI230805052S>

*Radical changes have been happening on the source side of the electricity system due to the rolling back of large-sized fossil-fueled power plants and the coming to the front of uncontrollable renewables. As a worldwide consequence, to ensure the permanent balance of the grid, even big-sized units have to be operated in load-following mode, including also nuclear power plants. This mode is conducted by the control system, which must also consider the side effects of this rather dynamic operating mode. In this report, we show up all components of such a control system, including the process model, structural integrity assessment, and control algorithm. All the aforementioned elements are discussed on the basis of a concrete example, and the resulting control behavior of the entire system is also shown. The results demonstrated that a significant reduction in the caused thermal stresses could be achieved while keeping the control quality practically unchanged.*

Key words: *fluid dynamics, heat transfer, stress-strain, strength of materials, aging, power plant, advanced control*

### Introduction

Electricity seems to be the most noble energy carrier. Its major bottleneck is well-known, as its storing is still not solved in an efficient way and appropriate amount. Consequently, a permanent balance between actual consumption and production is a must. Because the consumption side practically cannot be influenced, and because some uncontrollable elements have also been appearing on the production side, the rest of this side must satisfy the entire burden of controllability. So, the growing share of uncontrollable renewables, together with the decreasing amount of easy-to-control fossil-fueled power plants, result in the need for the load-following operation of rather big power generating units [1]. The difficulty is that such units were traditionally handled as permanent-load ones.

Nuclear power plants (NPP) are typical examples of this type, and they are characterized by outstandingly high relevance of security, economic, and ecological issues. Just because of these reasons, a basic question is whether they are capable of load-following operation at all. A high number of operational experiences answers this question definitely with yes. Germany

\* Corresponding author, e-mail: [szentannai.pal@ek-cer.hu](mailto:szentannai.pal@ek-cer.hu)

is an example where this was systematically investigated before the political decision to change the energy mix. This capability was clearly pointed out by many studies [2, 3], and several units were mentioned as examples that they were operated in this mode practically uninterruptedly throughout the entire year.

Worldwide experiences have also shown that the relative ramp rates of NPP are ranged close to those of conventional power plants, as visualized in the left diagram of fig. 1. Further, by also considering the generally very big rated power values of NPP, the same capabilities expressed in real ramp rates, that is, in MW per minutes, NPP definitely outperform the other power plants, as visible in the right diagram of fig. 1.

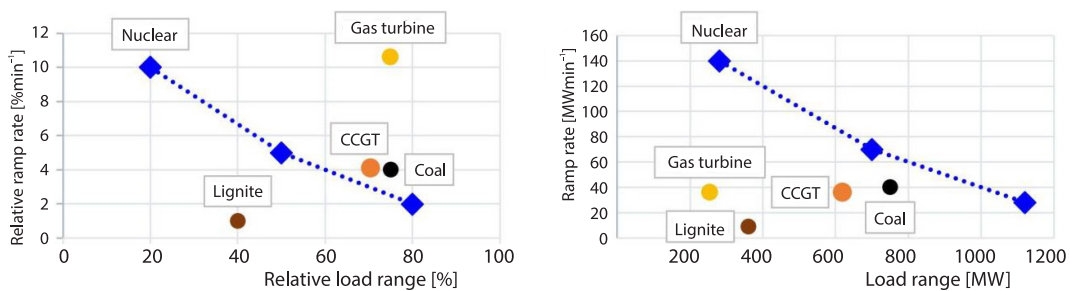


**Figure 1. Typical, practically allowable ramp rates and ranges of load changes of different power plant types; (a) diagram: relative values and (b) diagram: absolute values. For NPP, three different Ramp rate – Load range pairs are widely known and applied. Data from [4, 5]**

The newly required capability for this operation mode in the case of power plants is often called *manoeuvrability* (also *maneuverability*) [4, 6], which term comes from the aviation industry. Here, it is namely evident that faster control can be achieved at the expense of higher stress, especially on the wings. It also became evident that thoughtful control design may significantly reduce the stresses caused by the controller-managed transients – without causing any noticeable degradation in the control quality [7].

In a more common approach, investigating the stresses should be extended up to describing the material degradation (synonym: aging) they cause. This scientific area is the *structural integrity* (SI). In the case of the energy industry, especially for the rather relevant nuclear power plants, a systematic control design that incorporates also SI is still lacking.

In this paper, we formulate a generally applicable control structure together with all its necessary components for achieving load-following operation of NPP in such a way that also considers its side-effects on material aging.

The control structure is built up from the next basic elements:

- process model,
- model of SI phenomena, and
- the controller itself.

The only unusual component is the SI model, the rule and location of which are dual. It is a mathematical model, hence it is realized in the IT system, not in the power plant process, while, from the aspect of the controller, it belongs to the process to be controlled. The core of the current paper is divided into three main chapters to introduce the aforementioned three components. All these elements will be illustrated by concrete numerical figures referring to a typical (but not-nameable) case, the original design data of which are summarized in tab. 1.

**Table 1. Original design parameters of the nuclear power unit investigated in the current study**

Parameter	Value	Unit	Parameter	Value	Unit
Reactor thermal output	1 375	[MW]	Steam generator outlet pressure	44	[bar]
Reactor coolant volume flow rate	40 700	[m <sup>3</sup> per hour]	Steam generators' mass-flow rate	2 700	[tonne per hour]
Reactor coolant pressure	125	[bar]	Active core height	2.5	[m]
Reactor coolant inlet temperature	269	[°C]	Active core diameter	2.88	[m]
Reactor coolant outlet temperature	300	[°C]	Number of fuel assemblies	349	–

### Process modeling

A deep understanding of the process is a basic requirement for elaborating effective process control, according to the authors' sense. The knowledge about the process is generally expressed by a process model, which can be applied in multiple ways. It is a very useful tool for simulations throughout the development of the control strategy, on the one hand, and most control algorithms require a process model of a certain level, on the other hand.

Because the model is needed prior to the erection of the plant already, we propose the first-principle modelling approach. Further, because control systems may sense and act on discrete points only, the proposed model class is that of lumped models. Although the model is a theoretical (first principles) one, it contains several empirical functions, mostly for describing material properties. To make the model numerically effective, we did not directly build these functions into the computational model, instead, we applied polynomial approximations for the desired parameter ranges. We also recognized that most of these functions are rather close to linearity, see an example in fig. 2 and a summary in tab. 2. A typical example of the opposite end is the reactivity coefficient of the moderator influenced by the temperature and the boron concentration. Here, we found a polynomial approximation (in this case, a 2-D one), a satisfactory and, at the same time, effective description mode as well, fig. 3.

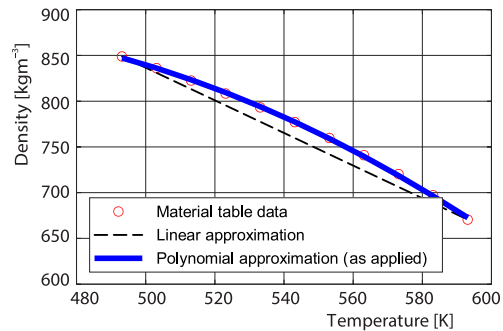


**Figure 2. Dependency of an example material property (density) as function of temperature, and its handling in the model; note that in this and most other cases, non-linearity is low within the ranges variables may take throughout the actual investigations**

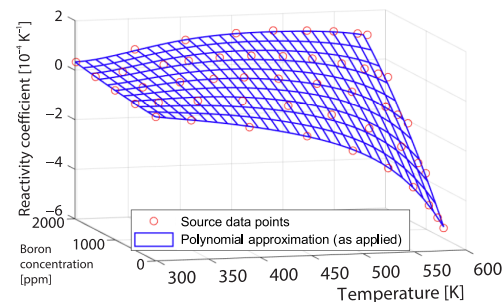


**Figure 3. The feedback effect of the boron concentration on core reactivity; this function of two independent variables is heavily non-linear; describing it and including it in the numerical model by polynomial approximation is also in this case an effective way**

**Table 2. Applied estimations in the model, their validity ranges and maximal relative errors**

Calculated variable	As function of	Validity range		Within the validity range	
		Lower limit	Upper limit	Max. relative error of linear span estimation	Max. relative error of the applied estimation
Specific internal energy of water at the primary pressure	Temperature [°C]	240	320	1.23%	0.15%
Saturation temperature of water	Pressure [bar]	40	52	0.08%	0.05%
Specific enthalpy of vaporization of saturated water	Pressure [bar]	40	52	0.06%	0.04%
Density of saturated water	Temperature [°C]	220	320	1.86%	0.23%
Specific enthalpy of heating of water up to saturation from the primary temperature	Pressure [bar]	40	52	1.01%	0.83%
Specific internal energy of saturated water	Pressure [bar]	40	52	0.15%	0.10%
Density of saturated vapor	Pressure [bar]	40	52	0.14%	0.10%
Density of water at the primary pressure	Temperature [°C]	220	320	2.35%	0.44%

The inputs of the model are the variables that also act in reality as inputs, that is, possible manipulated variables like control rod positions, main steam valve positions, and boron concentration. Similarly, all those variables are modeled as outputs that may be used as measured values for any control strategies like many temperatures in both the primary and secondary circuits, flow rates, neutron fluxes, water levels, *etc.*

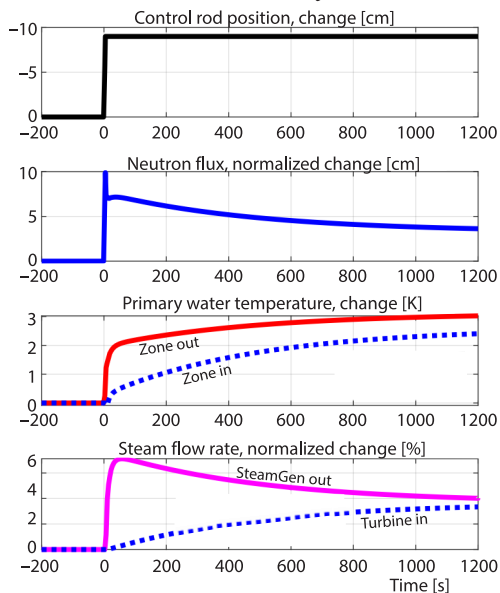


**Figure 4. Dynamical changes in some process variables as consequences of the withdrawal of the control rods; this simulation example shows that even the simple lumped model type (as discussed in this section) is capable of describing the complex dynamical behavior of the process in question**

The aforementioned dynamical, control-oriented model is a rather simple one. However, our extensive and comparative investigations show that this model is capable of reproducing even complex phenomena with adequate accuracy. As an example, consider the withdrawal of the control rods by a certain length and velocity. A few of the resulted responses are shown in fig. 4, from which the interesting dynamical behavior is visible, together with the well-known inherent self-regulating capability of this reactor type.

This figure also shows a general characteristic of this and all other simulations to be presented in this study. They are, namely, started from a steady-state operating point, which is clearly indicated by the steady values before the simulation start at  $t = 0$ . One operating point was chosen and used for this purpose, the main data of which are summarized in tab. 3.

**Table 3. Initial steady-state conditions for the dynamical simulations performed in this study**

Parameter	Value	Unit
Reactor thermal output	1 369	[MW]
Reactor coolant inlet temperature	265.8	[°C]
Reactor coolant outlet temperature	289.4	[°C]
Average coolant temperature in the primary loop	277.6	[°C]
Live steam pressure	41.0	[bar]
Live steam temperature	257.4	[°C]
Steam generators' mass-flow rate	2 685	[tonne per hour]
Control rod position	0.75	[m]

A programmed mathematical model is also capable of preliminary investigation of the process's non-linearity. We found that the investigated plant is very close to its linearized version within load deviations of 2-5%. This is a piece of important information as many practical load-change commands fall within this range. Hence, in these cases, a simple linear control algorithm can be fully adequate. Note that this also shows another requirement, namely, the need for a regular, state-dependent update of the linear model and controller.

### Structural integrity assessment

For considering the side-effects of the transient procedures managed by the controller, they must be included in the control scheme. As structural integrity issues are definitely the dominating ones among them [4, 5], our research focused on them. They cover two subsequent parts, stress-strain calculation and aging estimation.

### Stress-strain calculation

Instationary states cause thermal stresses in the structural materials. Highly relevant parts are the reactor pressure vessels of nuclear power plants due to their sizes, geometries, and also the fact that they are practically not replaceable. The most critical place within this area appears to be the nozzle region [8], hence our investigations focus on this, as shown in figs. 5 and 6. Because of the lack of possible direct measurements for gaining the actual stress values, *indirect measurements* are proposed to be applied. They are based on some traditionally available measurements, together with the calculation of the needed variables. This calculation is nothing else but a dynamic model, which we set up through an in-depth investigation. It started with a finite element analysis (FEA) around the most critical places. Based on fluid mechanical calculations, the heat transfer phenomena were numerically described, based on which the stress values inside the steel body could be obtained.

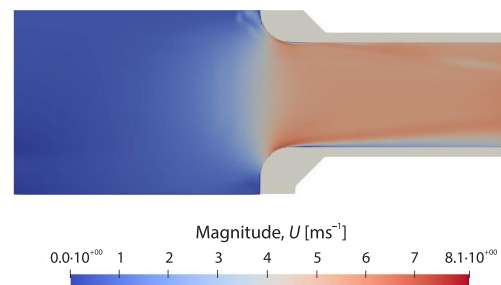


**Figure 5. Velocity field around the nozzle and in the pipe 100 seconds after the initial excitation, as an example of the results of the fluid dynamical investigations done by FEA**

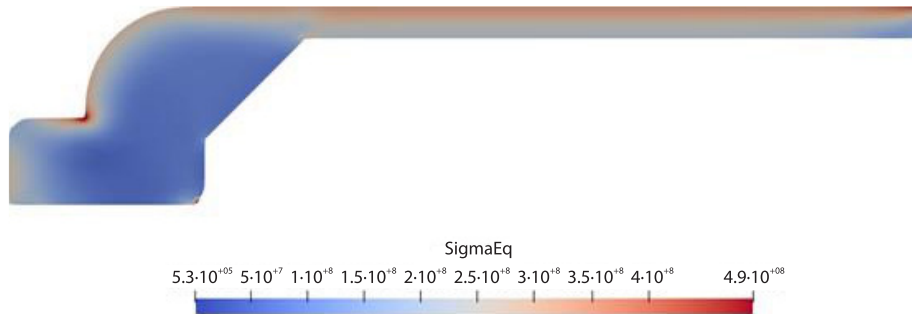


**Figure 6: Thermal stress field (von Mises stress values) within the solid body around the nozzle and the pipe, as an example of the results of the calculations on the strength of materials by FEA**

### Fluid dynamics

A lumped model of the entire power unit (as in section *Process modeling*) is capable of calculating the overall values around the points of interest. However, for local investigations, a deeper description is needed, which we gained via the multiscale approach. For this, we set up the gridded geometrical model of the most critical part. Our fluid-dynamical calculations are based on the Navier-Stokes eq. (1), supplemented by the continuity eq. (2):

$$\rho_f \left( \frac{\partial \mathbf{u}}{\partial t} + (\mathbf{u} \cdot \nabla) \mathbf{u} \right) = -\nabla p + \nabla \cdot \boldsymbol{\tau} + F_{\text{ext}} \quad (1)$$

$$\nabla \cdot (\rho_f \mathbf{u}) = 0 \quad (2)$$

where  $\mathbf{u}$  is the local fluid velocity vector,  $\rho$  – the density,  $p$  – the pressure,  $\boldsymbol{\tau}$  – the local shear stress tensor, and  $F_{\text{ext}}$  – summarizes the external forces.

In order to gain the dynamical description of the subprocess in question, we applied a well-defined input function (in this case, a simple step function), and the resulting velocity field was considered as the output function of time. One example at a selected time instance of the results is depicted in fig. 5. Based on this, the heat transfer coefficients can already be calculated as well. As visible, next to the wall, the liquid velocity is rather low, and the flow becomes heavily turbulent. Accordingly, the calculated heat transfer coefficient values are significantly higher in the turbulent region.

### Heat transfer

The fluid dynamical matters determine the actual conditions of heat transfer between fluids and solids, and also within the solid body.

The first term on the left-hand side of the energy eq. (3) for water describes the effect caused by the change of the liquid temperature,  $T_1$ , the second one, the convective heat transfer caused by the liquid velocity,  $\mathbf{u}$ , and the third one the heat transfer characterized by the liquid's thermal conductivity,  $\kappa_1$ . On the right-hand side, the two heat sources are shown as the  $\dot{Q}_{l-s}$  heat transfer and  $\dot{Q}_{\text{ext}}$  coming from the nuclear chain reaction. The energy eq. (4) for the solid phase is rather similar, with the sole difference that there is no flow in this case, hence the convective term should be omitted:

$$\rho_l c_l \frac{\partial T_l}{\partial t} + \rho_f c_l (\mathbf{u} \cdot \nabla) T_l - \nabla \cdot (\kappa_l \nabla T_l) = \dot{Q}_{l-s} + \dot{Q}_{\text{ext}} \quad (3)$$

$$\rho_s c_s \frac{\partial T_s}{\partial t} - \nabla \cdot (\kappa_f \nabla T_s) = -\dot{Q}_{l-s} \quad (4)$$

The overall results, that is, the field as function of time, is the input for the upcoming solid-mechanical calculations.

### Strength of materials

The equation on strength of materials:

$$\rho_s \dot{v} = \nabla \cdot \sigma + F_{\text{ext}} + 3K \alpha \nabla (T - T_{\text{ref}}) \quad (5)$$

The left-hand side describes the time-dependent local acceleration,  $\dot{v}$ . The terms on the right-hand side are the spatial distribution of the stress tensor,  $\sigma$ , the sum of external forces,  $F_{\text{ext}}$ , and the thermal expansion proportional to the spatial distribution of temperature,  $T$ . Here  $K$  is the bulk modulus, which is taken from the  $E$  Young modulus, and the  $\nu$  poisson coefficient:

$$3K = \frac{E}{1-2\nu} \quad (6)$$

Based on these equations, together with the *kinematic equation*, the *strain decomposition theorem*, and the *balance of momentum*, the thermal stresses within the body of the steel structural element can be calculated and visualized, as shown in fig. 6.

The stresses in the critical points are investigated then further – more precisely, their values as functions of time.

As a result of the local modelling introduced in the current section *Stress-strain calculation*, the stress values in the critical points are achieved as functions of time. Since the input of this series of finite element calculations was a well-defined input function (the step function of the liquid temperature), they can be considered as the step response functions. In order to turn them into an easy-to-implement dynamical component in a numerically cheap way, simple functions were fitted to them by means of a least-squares-based numerical optimum search. We found that as the transfer function, a rational fractional function with two poles and one zero gave absolutely satisfactory matching, as visible in fig. 7. Note that this type of transfer function also has a physical meaning as it corresponds to a fast initial upward edge and a slow relaxation in stress as the consequence of a stepwise temperature rise.

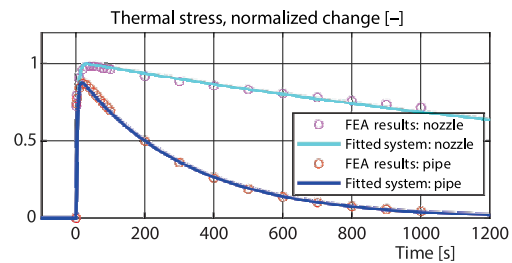


**Figure 7. Step response functions fitted to the outcomes of the stress-strain calculation of both nozzle and pipe, as introduced in section *Stress-strain calculation***

### Aging estimation

Stress in the solid material causes its aging. This is the next phenomenon to be modeled so that its output can be considered by the controller. A generally applied way is the so-called rain-flow counting method. Its major drawback is that it was developed and applied specifically for post-processing calculations. That is why, for the current application, it had to be turned into a

direct online method. For this, we followed the approach proposed by [9], throughout which we applied a function-fitting procedure for the class of time functions relevant to the current study.

As the first test of the aforementioned direct online rainflow-counting method, we checked the consequences of some control actions. The three columns in fig. 8 show the achievement of the same load changes of about 40% decrease. The only difference is that the actuator actions were carried out in three different ways. The third diagrams from the top show that different control actions resulted in different absolute peak stress values. Further, the bottom diagrams show that the damage rate diagrams and also their integrals, the caused damage values differ markedly.

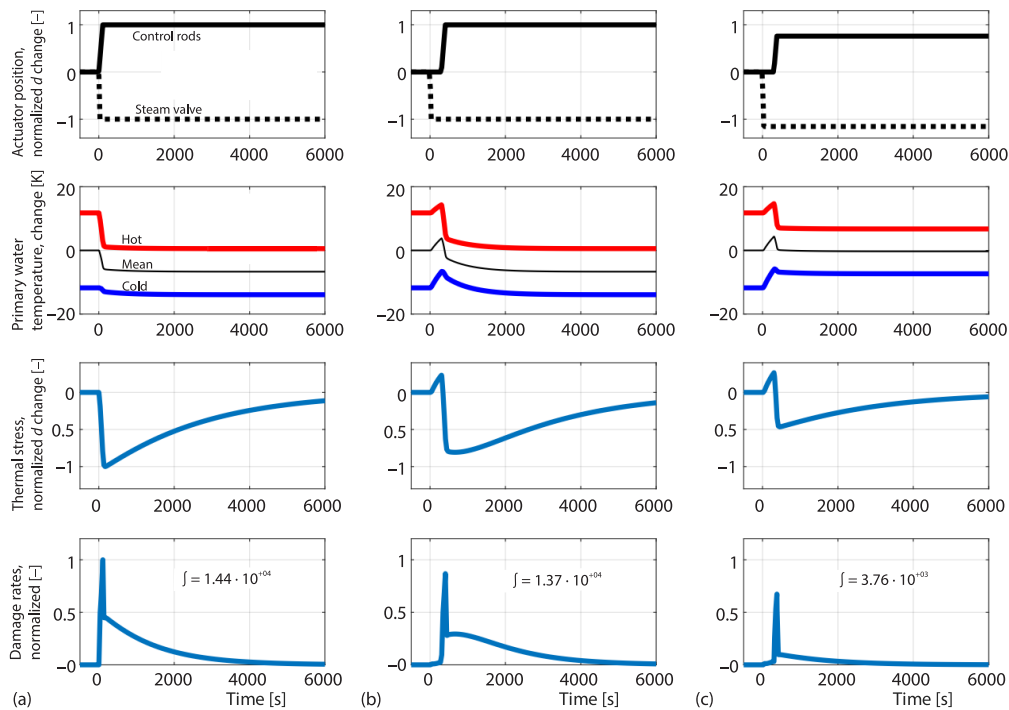


**Figure 8.** The same plant load decrease was carried out by three different arbitrary control sequences, as shown in columns (a)-(c). As visible in the third row of diagrams, the maximum absolute thermal stresses differ markedly from case to case. Further, the bottom diagrams show the caused damage rates, the integrals of which do also differ significantly

### Controller design

The preliminary investigations show, see fig. 8, that the control algorithm may significantly influence the transient's effect on material aging, hence the technically allowable lifetime of critical equipment – even while not influencing the control quality. However, formulating the latter criteria is still not evident.

In the case of power plants, the major expectations refer to the electrical power (the actual load) the unit has to deliver to the grid. For steady-state operation mode, the corresponding legal text cannot be too complicated, however, for load-following operation, generally, it is. The reason is obvious as the expectations must be formulated as functions of time, and the history of the load command must also be considered. A general mistake in representing the

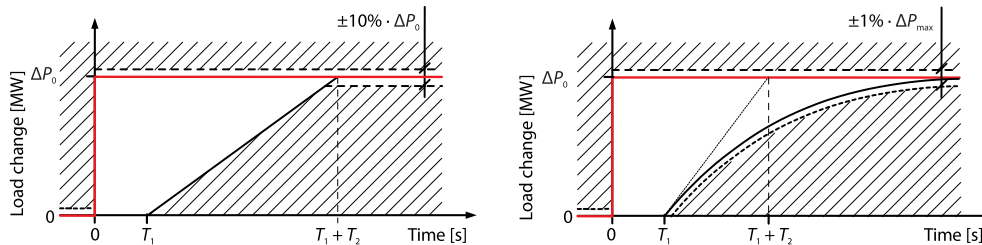


**Figure 9.** The two typical criterion diagrams to be satisfied by the plant control throughout load changes. Note that these representations are the results of careful interpretations of the contractual texts. For control design, it is crucial to extract and use these diagrams instead of believing a must for a strict ramp-follow

contractual requirement is to believe that a strict following of a given line or ramp is a must. In fact, there is much more freedom. In fig. 9, we depicted the two most general, real, time-dependent expectations valid in the European electricity systems.

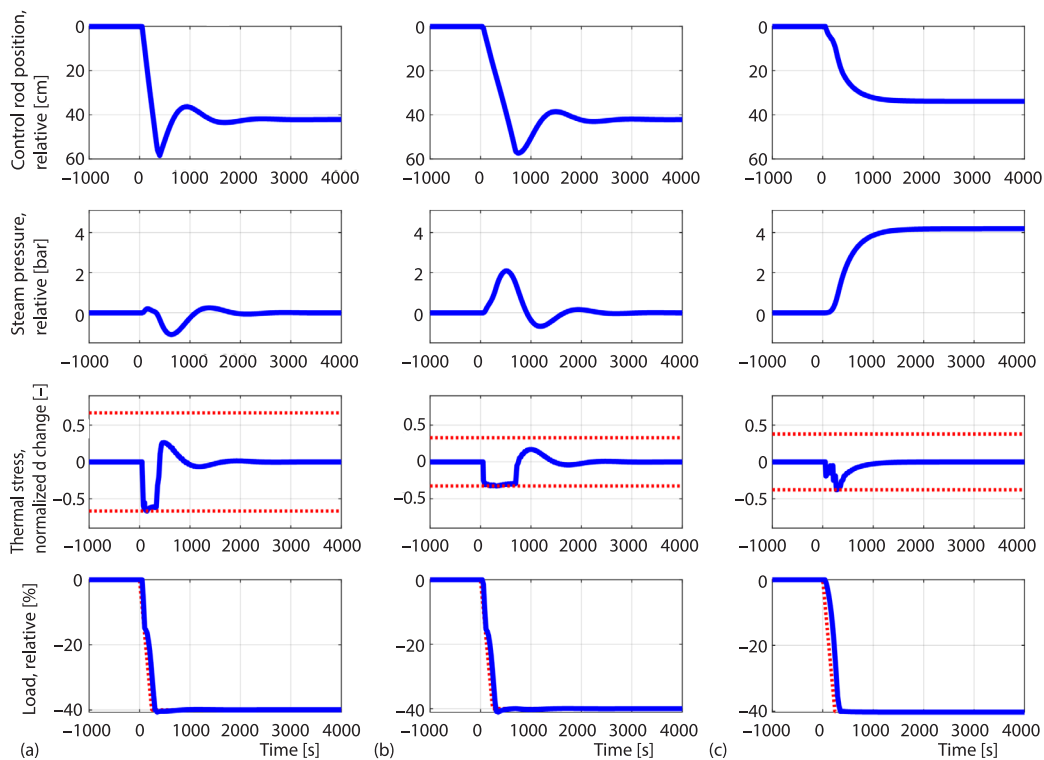


**Figure 10.** Different control actions and consequences for carrying out the same load-decreasing procedure; (a) constraint was set for the thermal stress, which was kept, as visible in the third diagram, (b) narrower stress range was allowed, which could be achieved by the controller by allowing higher fluctuation in the main steam pressure (compare the second diagrams from the top), (c) even the steady-state steam pressure was not forced back to its original value, which practically corresponds to another strategy of the classical control philosophy. Observe the practically unchanged control qualities and the control actions for slowing the rod movements in some periods without slowing down the entire procedure

Control theory offers a wide range of control algorithms, which are capable of considering all aforementioned characteristics of the job including this play-field and the plant dynamical behavior, together with the SI effects, as outlined previously. Advanced model-based control algorithms are also mostly capable of considering the SI behavior either as components of the cost function, damage rates, *e.g.*, or as constraints, *e.g.* stresses.

The latter case is demonstrated in fig. 10, the columns of which represent the results of three different MPC settings with various stress constraints and weighting factors for the main steam pressure. As visible, the controller was able to slow down the process – but just where it was convenient, not generally! Further, it has happened without any noticeable loss in the control quality.

### Conclusion

Several worldwide trends do further urge also NPP to enable load-following operation mode. This can only be realized by applying control algorithms that consider, besides control quality, also the SI consequences. All components of such a control structure were introduced and successfully tested in the current research.

### Acknowledgment

The kind help of Dr. A. Horvath, DSc. J. Gado, DSc Z. Hozer, and J. S. Janosy, as well as L. Tatar, and D. Antok are gratefully acknowledged.

### Contribution

**P. Szentannai:** Conceptualization, Methodology, Supervision, Investigation, Writing – original draft, review & editing. Dynamical modeling of the plant; optimization, control strategy. **T. Szucs:** Investigation: FEA stress–strain calculations. Writing – original draft, review. **B. Pudleiner:** Investigation: aging calculations. Reviewing **T. Fekete:** Supervision, Reviewing.

### Nomenclature

$c$  – specific heat, [ $\text{Jkg}^{-1}\text{s}^{-1}$ ]  
 $E$  – Young's modulus, [Pa]  
 $F$  – force, [N]  
 $K$  – stress intensity factor, [ $\text{Pa}\cdot\text{m}^{0.5}$ ]  
 $P$  – load, [W]  
 $p$  – pressure, [Pa]  
 $\dot{Q}$  – heat flux, [W]  
 $T$  – temperature, [K]  
 $T$  – time constant, [second]  
 $t$  – time, [second]  
 $\mathbf{u}$  – velocity vector, [ $\text{ms}^{-1}$ ]  
 $\dot{\mathbf{v}}$  – local accelerator vector, [ $\text{ms}^{-2}$ ]

### Greek letters

$\alpha$  – coefficient of linear expansion, [ $\text{mK}^{-1}$ ]  
 $\kappa$  – thermal conductivity, [ $\text{Wm}^{-1}\text{K}^{-1}$ ]  
 $\nu$  – Poisson's ratio, [–]  
 $\rho$  – density, [ $\text{kgm}^{-3}$ ]  
 $\sigma$  – stress tensor, [Pa]  
 $\tau$  – shear stress tensor, [Pa]

### Subscripts

ext – external  
 $\ell$  – liquid phase  
 ref – reference  
 s – solid phase

### References

- [1] Marusic, A., *et al.*, Increasing Flexibility of Coal Power Plant by Control System Modifications, *Thermal Science*, 20 (2016), 4, pp. 116-1169
- [2] Ludwig, H., *et al.*, Lastwechselfähigkeiten deutscher KKW (in German), Load cycling capabilities of German Nuclear Power Plants (NPP), *Jahegang*, 55 (2010), 8/9
- [3] Grunwald, R., Caviezel, C., Load-Following Capability of German Nuclear Power Plants, *Summary*, 2017
- [4] \*\*\*, IAEA, Non-Baseload Operation in Nuclear Power Plants: Load Following and Frequency Control Modes of Flexible Operation. International Atomic Energy Agency, [https://www-pub.iaea.org/MTCD/Publications/PDF/P1756\\_web.pdf](https://www-pub.iaea.org/MTCD/Publications/PDF/P1756_web.pdf), 2018

- [5] Kosowski, K., Diercks, F., Quo Vadis, Grid Stability, Title of the German translation: *Quo vadis, Netzstabilität*, 66 (2021), 2, 11
- [6] \*\*\*, NEA, Technical and Economic Aspects of Load Following with Nuclear Power Plants – OECD 2011. Nuclear Energy Agency, Organisation for Economic Co-operation and Development, <https://www.oecd-nea.org/ndd/reports/2011/load-following-npp.pdf>, 2011
- [7] Szentannai, P., Fekete, T., Integrated Optimization of Process Control and Its Effect on Structural Integrity – A Systematic Review, *Engineering Failure Analysis*, 140 (2022), 106101
- [8] Li, Y., *et al.*, Engineering Critical Assessment of RPV with Nozzle Corner Cracks under Pressurized Thermal Shocks, *Nuclear Engineering and Technology*, 52 (2020), 11, pp. 2638-2651
- [9] Loew, S., *et al.*, Direct Online Rainflow-Counting and Indirect Fatigue Penalization Methods for Model Predictive Control, *Proceedings*, 18<sup>th</sup> European Control Conference (ECC), Naples, Italy, 2019, pp. 3371-3376